Airfoil Thickness Effects on the Thrust Generation of Plunging Airfoils

Meilin Yu,* Z. J. Wang,† and Hui Hu‡
Iowa State University, Ames, Iowa 50011

A numerical study was conducted to investigate the effects of airfoil thickness on the thrust generation of plunging airfoils and to assess the contributions of pressure and viscous forces in flapping propulsion. A series of NACA symmetric airfoils with thickness ratio ranging from 4.0% to 20.0% of the airfoil chord length were used in the present study to undertake a same sinusoid plunging motion at a low Reynolds number of $Re = 1200$ with the plunging Strouhal number $Str = 0.45$ and reduced frequency $k = 3.5$. It was found that the thickness of the airfoils would affect the evolution of the unsteady vortex structures around the plunging airfoils significantly, even though the airfoils were set to undertake the same plunging motion. The different behaviors of the unsteady vortex structures shedding from the airfoils with different thickness were found to cause dramatic changes to the resultant aerodynamic force acting on the plunging airfoils. For a thick plunging airfoil with its thickness ratio greater than 9.0%, pressure force was found to play a dominant role in the thrust generation, and viscous force would be almost negligible and contribute mainly to drag production. It confirms that the traditional inviscid model of the Knoller–Betz effect (i.e., ignoring viscous effect) can be used to explain many phenomena associated with flapping propulsion. A new finding of the present study is the substantial contribution of viscous force to the thrust generation for thin plunging airfoils (i.e., the thickness ratio less than 8.0%). Viscous force was found to become thrust-producing, instead of drag-producing, and it played a nonnegligible role in the thrust generation for the thin airfoils (i.e., viscous force would produce up to 20.5% of the total thrust for NACA0004 airfoil in the present study). The role change of viscous force in the thrust generation of the plunging airfoils was found to be closely related to the variations of the dynamics of the unsteady vortex structures around the plunging airfoils.

Introduction

MICRO air vehicles (MAVs) have been one of the most active research topics in the aerospace engineering community in recent years. The miniaturized aircraft is expected to open up new opportunities for surveillance-like missions, especially in hazardous environments inaccessible to ground vehicles. Among different MAV designs, flapping-wing-based designs stand out with high efficiency and excellent maneuverability, as demonstrated by the natural fliers such as birds and insects. It has long been realized that steady-state aerodynamics does not accurately account for the aerodynamic forces produced in flapping flight. This has prompted extensive studies to elucidate the fundamental mechanism of flapping flight to produce enough aerodynamic forces needed for propulsion and maneuvering. Knoller [1] and Betz [2] are among the first to propose an invisid theory, which is known as the Knoller–Betz effect, to explain why a flapping wing can generate thrust in flapping motion. Katzmayr [3] provided the first experimental verification of the Knoller–Betz effect by placing a stationary wing into a sinusoidally oscillating airflow. Ober [4] provided additional theoretic explanations and calculations to confirm Katzmayr's experimental results. Much progress has been made since then to uncover the underlying physics of flapping propulsion [5–15].

Although many important findings have been derived through those previous studies, much work is still needed for a better understanding of flapping propulsion for the optimum design of flapping-wing-based MAVs. For example, while birds and insects flap their thin wings to fly (i.e., wing thickness is only a few percent of the chord length), much thicker airfoils (airfoil thickness >10% of chord length) were usually used in previous studies to reveal the underlying physics of flapping flight [6–12]. Although numerous experimental and numerical studies have been conducted recently to investigate the effects of kinematic parameters of flapping motions (such as the flapping frequency, amplitude, and phase difference between plunging and pitching motions) on the thrust generation and propulsive efficiency, the influence of airfoil thickness on flapping propulsion has not yet been fully explored [10]. Furthermore, while the inviscid model of Knoller–Betz effect (i.e., ignoring viscous effect) has been used widely to explain many phenomena associated with flapping propulsion [8–10], the role of viscous force in flapping propulsion is still poorly understood. Many fundamental questions still remain to be answered, such as "Are viscous effects negligible for flapping propulsion under all conditions?" and "Although viscous force is known to be usually drag-producing, can it ever make a positive contribution to the thrust generation in flapping propulsion?"

In this short paper, we report a numerical study to investigate the effects of airfoil thickness on the thrust generation of plunging airfoils and to assess the contribution of viscous force to the thrust generation in flapping propulsion. A series of commonly used symmetric NACA airfoils with thickness ranging from 4 to 20% of the chord length were used to undertake the same plunging motion at a low Reynolds number of $Re = 1200$. The behavior of the unsteady vortex structures around the plunging airfoils and the resultant aerodynamic forces acting on the plunging airfoils were compared quantitatively to reveal the underlying physics related to flapping propulsion. The contribution of viscous force on the thrust generation in flapping propulsion was also examined in detail based on the quantitative comparison.

*Graduate Student, Department of Aerospace Engineering.
†Professor, Department of Aerospace Engineering. Associate Fellow AIAA.
‡Associate Professor, Department of Aerospace Engineering; huhui@iastate.edu. Associate Fellow AIAA.

Numerical Method and Studied Parameters

In the present study, a high-order spectral difference method with dynamic unstructured grids was used for the numerical simulation.

The governing equations for the fluid flow are the unsteady Navier–Stokes equations in a conservation form, which can be expressed as

$$\frac{\partial Q}{\partial t} + \frac{\partial F}{\partial x} + \frac{\partial G}{\partial y} + \frac{\partial H}{\partial z} = 0 \qquad (1)$$

Herein, $Q = (\rho, \rho u, \rho v, \rho w, E)^T$ are the conservative variables; ρ is the fluid density; u, v, and w are the Cartesian velocity components; and E is the total initial energy. F, G, H are the total fluxes including both the inviscid and viscous flux vectors, i.e., $F = F^i - F^v$, $G = G^i - G^v$ and $H = H^i - H^v$. Detailed formulas for the fluxes can be found in Yu et al. [15]. With the assumption that the fluid obeys the perfect gas law, the pressure is related to the total initial energy by $E = p/(\gamma - 1) + \frac{1}{2}\rho(u^2 + v^2 + w^2)$, which closes the solution system.

To achieve an efficient implementation, a time-dependent coordinate transformation from the physical domain (t, x, y, z) to the computational domain (τ, ξ, η, ζ) is applied on Eq. (1), which is

$$\frac{\partial \tilde{Q}}{\partial \tau} + \frac{\partial \tilde{F}}{\partial x} + \frac{\partial \tilde{G}}{\partial y} + \frac{\partial \tilde{H}}{\partial z} = 0 \qquad (2)$$

where

$$\begin{cases} \tilde{Q} = |J|Q \\ \tilde{F} = |J|(Q\xi_\tau + F\xi_x + G\xi_y + H\xi_z) \\ \tilde{G} = |J|(Q\eta_\tau + F\eta_x + G\xi_y + H\eta_z) \\ \tilde{H} = |J|(Q\zeta_\tau + F\zeta_x + G\zeta_y + H\zeta_z) \end{cases} \qquad (3)$$

Herein, $\tau = t$ and $(\xi, \eta, \zeta) \in [-1, 1]^3$ are the local coordinates in the computational domain. In the transformation shown previously, the Jacobian matrix J takes the following form:

$$J = \frac{\partial(x, y, z, t)}{\partial(\xi, \eta, \zeta, \tau)} = \begin{pmatrix} x_\xi & x_\eta & x_\zeta & z_\tau \\ y_\xi & y_\eta & y_\zeta & y_\tau \\ z_\xi & z_\eta & z_\zeta & z_\tau \\ 0 & 0 & 0 & 1 \end{pmatrix} \qquad (4)$$

Note that the grid velocity $\vec{v}_g = (x_t, y_t, z_t)$ is related with $(\xi_\tau, \eta_\tau, \zeta_\tau)$ by

$$\begin{cases} \xi_\tau = -\vec{v}_g \cdot \nabla \xi \\ \eta_\tau = -\vec{v}_g \cdot \nabla \eta \\ \zeta_\tau = -\vec{v}_g \cdot \nabla \zeta \end{cases} \qquad (5)$$

In the present study, H-refinement (grid refinement) and p-refinement studies were conducted at first to determine the suitable grid and numerical accuracy. Based on the investigations, a third-order-accurate scheme with a medium mesh was chosen. A time-refinement study was also performed to determine a reasonable nondimensional time step for the present study. Further information about the implementation of the method described previously for the numerical simulation of the unsteady flows around flapping airfoils as well as the validation of the simulation results against experimental data is available in [15].

The airfoils used in the present study are a series of symmetric NACA airfoils, i.e., NACA0004, NACA0006, NACA0009, NACA0012, and NACA0020 airfoils. The airfoils were set to undertake a plunging motion, which can be expressed as $y = A \sin(2\pi f t)$, where f is the flapping frequency, and A is the plunging amplitude. The Reynolds number Re, based on the airfoil chord length C and the freestream velocity V_∞, was set to be 1200 for the present study, i.e., $Re = \rho V_\infty C/\mu = 1200$, which is well within the insect flight regime. Strouhal number $Str = 2fA/V_\infty$ and reduced frequency $k = 2\pi f C/V_\infty$ are the most commonly used nondimensional parameters to characterize the kinematics of flapping airfoils/wings. In the present study, the Strouhal number of the plunging airfoils was chosen to be 0.45, i.e., $Str = 0.45$. The reduced frequency of the plunging motion was set to be 3.5, i.e., $k = 3.5$. It

has been suggested that the wake flow downstream of a flapping airfoil/wing can be characterized as drag-producing, neutral, or thrust-producing, depending on the flapping frequency and stroke amplitude [6–14]. Based on the findings of the previous work of Jones et al. [8] and Lewin and Haj-Hariri [12], with the kinematic parameters used in the present study, the wake flows downstream the plunging airfoils should be thrust-producing, which was confirmed by the numerical simulation results of the present study.

Results and Discussions

Figures 1 and 2 display the typical behaviors of the unsteady vortex structures around a thick airfoil (e.g., NACA0020) and a thin airfoil (e.g., NACA0004) in a plunging cycle. The flow pattern around the plunging airfoils at such a relatively large Strouhal number (i.e., $Str = 0.45$) was found to be featured mainly by the periodic shedding of leading-edge vortices (LEVs) and trailing-edge vortices (TEVs) as well as the interactions among LEVs, TEVs, and plunging airfoils, which agrees with those reported by Lewin and Haj-Hariri [12]. It is also observed that, even though the airfoils were set to undertake the same plunging motion, the evolutions of the unsteady LEVs and TEVs around the plunging airfoils were found to vary significantly due to the thickness differences of the airfoils. As shown in Fig. 1, for the thick airfoil case, the LEVs shed from the airfoil leading edge were found to travel downstream along with the freestream continuously and then interact with the TEVs further downstream. Similar behavior of the LEVs was also reported by Ashraf et al. [10] in their study of the vortex structures around a plunging NACA0012 airfoil. However, for the thin airfoil (e.g., NACA0004) as shown in Fig. 2, instead of traveling downstream along with the freestream continuously, the LEVs over the lower (or upper) surface of the airfoil were found to stay close to the airfoil leading edge during the entire downstrokes (or upstrokes) of the plunging motion. After being stretched seriously, the LEVs were found to move against the freestream around the sharp airfoil leading edge and shift to the upper (or lower) side of the airfoil during the subsequent upstrokes (or downstrokes). Such phenomena were also found by Lewin and Haj-Hariri [12] and were named as LEV circumnavigation. Associated with the different behaviors of the LEVs around thick and thin airfoils, the flow patterns and the resultant aerodynamic forces acting on the plunging airfoils were also found to vary dramatically.

Figure 3 shows the pressure distributions and velocity vector fields (only 2% of the vectors were shown) around NACA0020 and NACA0004 airfoils at the same plunging phase angle of $\Phi = 180$ deg. It can be found that, for a thick airfoil such as NACA0020, corresponding to the rolling up of the LEVs on the airfoil upper (or lower) surface during the downstrokes (or upstrokes) of the plunging motion, a region with relatively low pressure was found on the airfoil upper (or lower) surface near the airfoil leading edge as shown in Fig. 3a, which is favorable for the thrust generation. The region with relatively low pressure was found to separate from the airfoil surface and move downstream as the LEVs shed from the airfoil leading edge and travel downstream. However, for a thin airfoil as shown in Fig. 3b, associated with the LEV circumnavigation described previously, low-pressure regions were found to exist on both the upper and lower surfaces, and the low-pressure regions would remain near the airfoil leading edge during almost the whole plunging cycle. Furthermore, the LEV circumnavigation was also found to induce strong reversed flows on both the upper and lower surfaces near the leading edge of the thin airfoils. Corresponding to the strong reversed flows near the airfoil leading edge, the viscous force acting on the upper and lower surfaces of the thin airfoil could actually be thrust-producing, instead of being drag-producing. The interesting finding can be revealed more quantitatively in the analysis of the resultant aerodynamic forces acting on the plunging airfoils.

Based on the distributions of pressure and viscous forces on the surfaces of the plunging airfoils, the resultant aerodynamic forces acting on the plunging airfoils in the term of thrust coefficient $C_T = \text{Thrust}/(0.5\rho V_\infty^2 S)$ were determined. Figure 4 shows the histories of the thrust coefficients of the five plunging airfoils
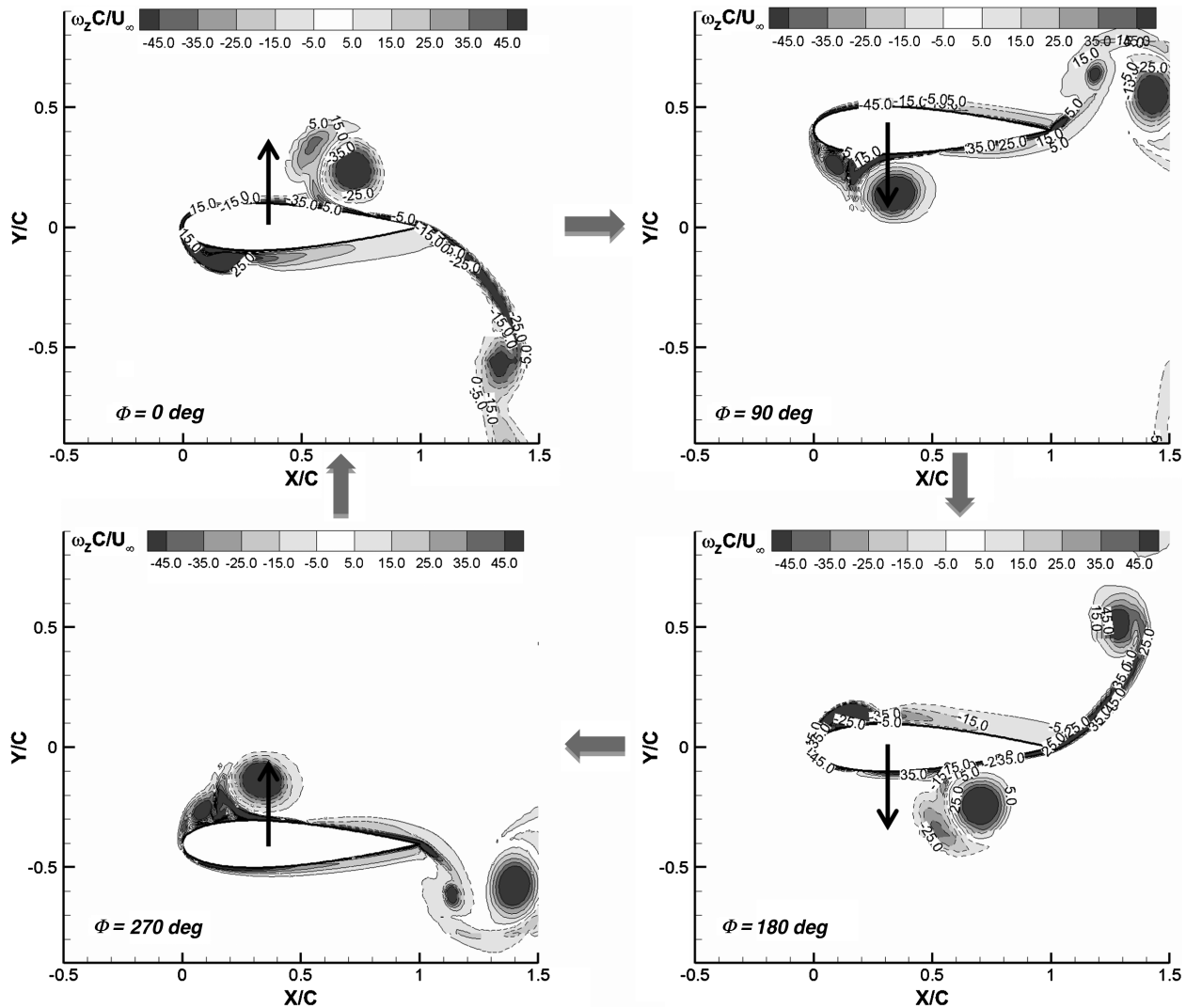
Fig. 1   Evolution of the unsteady vortex structures around NACA0020 airfoil in a plunging cycle.

investigated in the present study. It can be seen that, although the thrust coefficients of the plunging airfoils were found to fluctuate greatly in each plunging cycles, the fluctuating amplitude of the thrust coefficients decreases as the thickness of the plunging airfoil decreases. Although all the airfoils were set to undertake the same periodic plunging motion, only the thrust coefficients of the thicker airfoils (e.g., NACA0020 and NACA0020 airfoils) were found to be periodic, as expected. The thrust coefficients of the thinner airfoils (e.g., NACA0004 and NACA0006 airfoils) were found to become aperiodic even though the plunging motion of the airfoils is periodic. The aperiodic behavior of the flowfield around a plunging airfoil was also reported by Lewin and Haj-Hariri [12] with an elliptical airfoil plunging at a similar Strouhal numbers (e.g., $Str \approx 0.48$) as that of the present study. It should also be noted that, for the thicker airfoils (e.g., NACA0012 or NACA0020), while the resultant aerodynamic force acting on the plunging airfoils were found to be thrust-producing for most of the time in each plunging cycles (i.e., thrust coefficient being positive), the resultant aerodynamic force could also become drag-producing (i.e., thrust coefficient becoming negative) at some phase angles. However, the thrust coefficients of the thinner airfoils (e.g., NACA0004 or NACA0006) were found to be positive almost in the entire plunging cycles, which indicates that almost no drag was experienced by the thinner airfoils during the plunging motion. This is believed to be closely related to the LEV circumnavigation to maintain low-pressure regions and reverse flows near the leading edges of the thinner airfoils.

To assess the role of viscous force in the thrust generation of flapping propulsion, the total thrusts acting on the plunging airfoils

were decomposed into two parts, i.e., one part contributed from pressure force, $T_p = \int p n_x \, ds$, and the other from the viscous force, $T_v = \int (\sigma_{xx} n_x + \sigma_{xy} n_y + \sigma_{xz} n_z) \, ds$, where σ denotes the viscous stresses. Figure 5 shows the comparisons of the total thrust coefficients (i.e., considering the contributions from both pressure and viscous forces) and the thrust coefficients based on the contribution from pressure force only (i.e., ignoring the viscous forces) for NACA0020 and NACA0004 airfoils. Although the profiles in solid lines represent the total thrust coefficients, the profiles in dashed lines indicate the results based on the contribution from pressure force only. The differences between the solid and dashed lines would represent the contribution of viscous force on the thrust generation. It can be seen clearly that, compared with viscous force, pressure force was found to play a dominant role in the thrust generation of flapping propulsion. It is also observed that the differences between the solid and dashed lines were found to become larger for the thinner airfoil (e.g., NACA0004), compared with those for the thicker airfoil case (e.g., NACA0020). This indicates that the effects of viscous force on the thrust generation in flapping propulsion would become stronger for the thinner airfoils.

To reveal the contribution of viscous force on the thrust generation of the plunging airfoils more clearly and quantitatively, the averaged total thrust coefficients of the plunging airfoils, $\langle C_T \rangle$, and the contributions from pressure force, $\langle C_{T_P} \rangle$, and viscous force, $\langle C_{T_V} \rangle$, over plunging cycles were calculated. As revealed clearly from the results listed in Table 1, the averaged thrust coefficients of the plunging airfoils vary significantly as the airfoil thickness changes. With the plunging kinematic parameters and the airfoil thickness
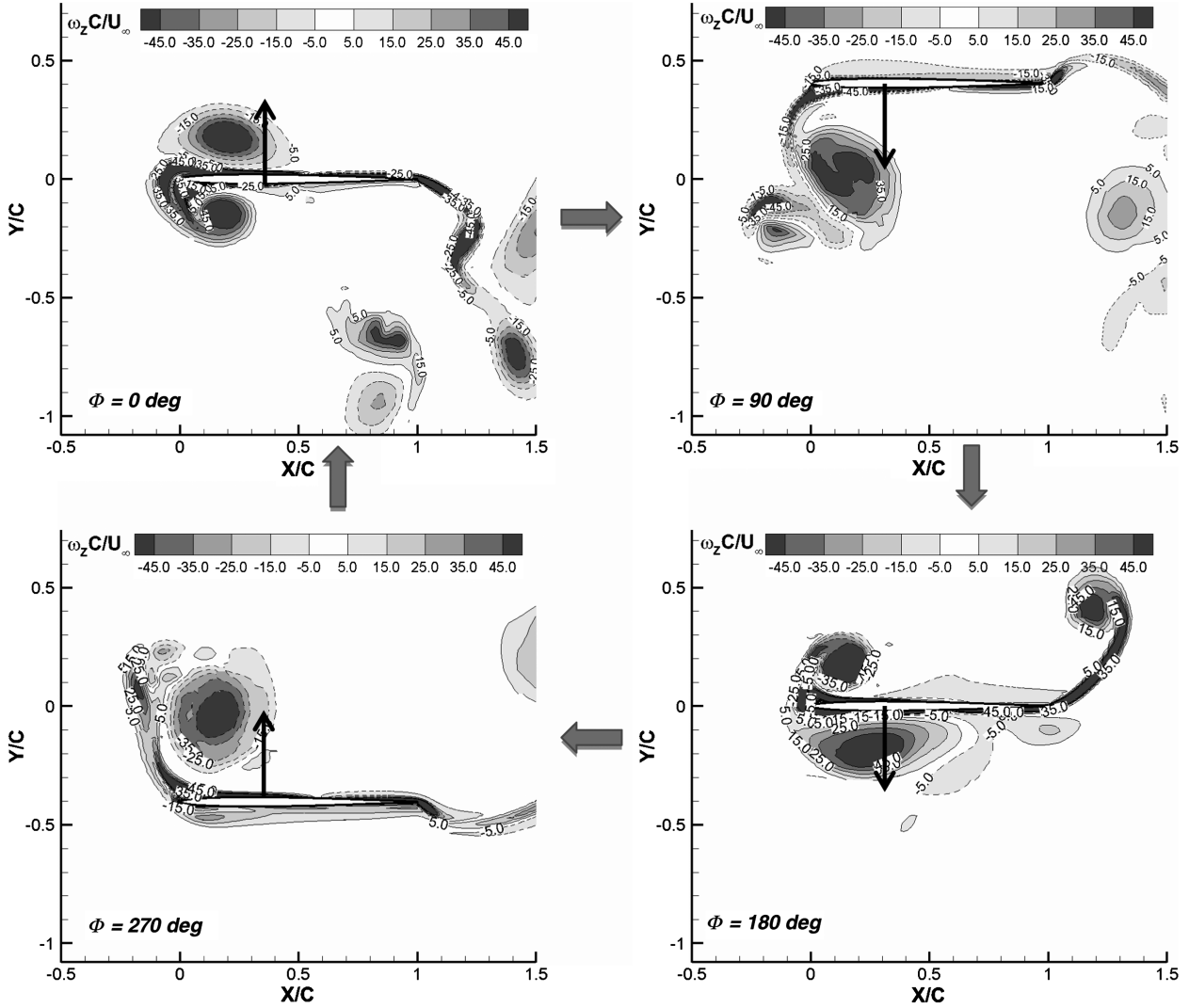
Fig. 2   Evolution of the unsteady vortex structures around NACA0004 airfoil in a plunging cycle.

range used in the present study, a thicker airfoil was found to generate a larger averaged thrust when undertaking a same plunging motion. The finding was found to agree with the conclusion reported by Ashraf et al. [10]. The results shown in Table 1 also confirmed that

pressure force would play a dominant role in the thrust generation of flapping propulsion. For the thicker airfoils (e.g., NACA0012 and NAC0020 airfoils), viscous force was found to be mainly drag-producing, and its effect was found to be very small (~2.0%), which
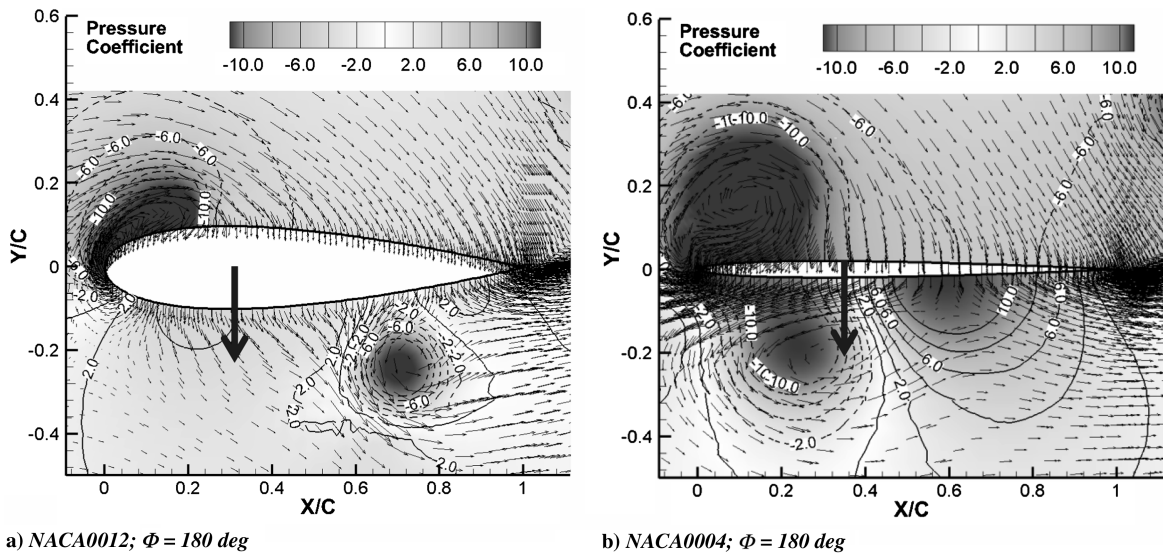
a) *NACA0012; $\Phi = 180$ deg*   b) *NACA0004; $\Phi = 180$ deg*

Fig. 3   Comparison of the pressure distributions and velocity fields around NACA0020 and NACA0004 airfoils at the phase angle of $\Phi = 180$ deg in the plunging motion.
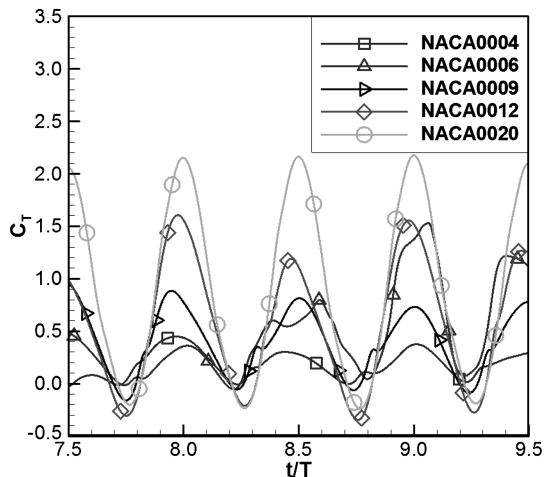
Fig. 4 Histories of the thrust coefficients of the NACA symmetrical airfoils in plunging motion.
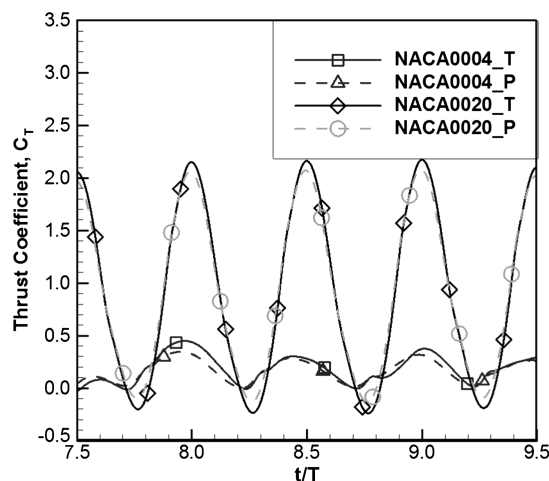

Fig. 5 Comparison of the total thrust coefficients of the plunging airfoils and the contributions from pressure force only.

is negligible. The finding can be used to explain why the traditional inviscid model of Knoller–Betz effect (i.e., ignoring the viscous effect) can be used to explain many phenomena associated with flapping propulsion. The drag-producing nature of viscous force for thick airfoils was found to agree with the results reported by Wang [11]. More interestingly, as revealed from the results given in Table 1, viscous force becomes thrust-producing, instead of drag-producing, for the thinner airfoils (e.g., NACA0006 and NACA0004). The contribution of viscous force to the thrust generation in flapping flight was found to become more and more substantial as the thickness of the plunging airfoil decreases (i.e., 13.6% for NACA0006 and up to 20.5% for NACA0004). This is believed to be closely related to the existence of reverse flows near the leading edges on both sides of the airfoil surfaces during almost whole plunging cycles for the thinner airfoils, as shown clearly in Fig. 3.

Table 1   Averaged total thrust coefficients $\langle C_T \rangle$ and the contributions from the pressure force $\langle C_{T_P} \rangle$ and viscous force $\langle C_{T_v} \rangle$

Airfoil	$\langle C_T \rangle$	$\langle C_{T_P} \rangle$	$\langle C_{T_v} \rangle$	$\langle C_{T-V} \rangle / \langle C_T \rangle$
NACA0004	0.261	0.208	0.053	20.5%
NACA0006	0.384	0.332	0.052	13.6%
NACA0009	0.410	0.421	−0.011	−2.6%
NACA0012	0.573	0.584	−0.011	−1.9%
NACA0020	0.920	0.937	−0.017	−1.9%

Conclusions

A numerical study was conducted to investigate the effects of airfoil thickness on the thrust generation of plunging airfoils and to assess the contribution of viscous force to flapping propulsion. A series of commonly-used NACA symmetric airfoils were used in the present study to undertake a same plunging motion at a low Reynolds number of $Re = 1200$ with the plunging Strouhal number $Str = 0.45$ and reduced frequency $k = 3.5$. It was found that, even though the airfoils were set to undertake the same plunging motion, the evolutions of the vortex structures around the plunging airfoils and the resultant aerodynamic forces acting on the airfoils varied dramatically due to the difference in airfoil thickness.

Although the leading-edge vortices (LEVs) of the thicker airfoils (e.g., >9.0% thickness ratio for the present study) were found to shed periodically and travel downstream along with the freestream continuously, LEV circumnavigation was found for the thinner airfoils (e.g., <9.0% thickness ratio) with LEVs stretched and remaining near the airfoil leading edges for most of time in the plunging cycles. Associated with the LEV circumnavigation, low-pressure regions and reverse flows were found to remain near the leading edge on both sides of the airfoils during almost whole plunging cycles for the thinner airfoils. The different behaviors of the LEVs for the thick and thin airfoils were found to affect the resultant aerodynamic force acting on the plunging airfoils dramatically. Although the thrust generation of the plunging airfoils with larger thickness was found to be periodic as expected, the thrust generation of the thin airfoils was found to become aperiodic even though the plunging motion is periodic.

The present study also revealed that pressure force plays a dominant role in the thrust generation of the plunging airfoils. As expected, viscous force contributes mainly to drag production, and its effect is almost negligible for the airfoils with relatively large thickness, which explains why the traditional inviscid model of Knoller–Betz effect (i.e., ignoring the viscous effect) can be used to explain many phenomena associated with flapping propulsion. Another important finding of the present study is the substantial contribution of viscous force to the thrust generation for thin airfoils. The viscous force was found to become thrust-producing, instead of drag-producing, and it played a nonnegligible role in the thrust generation for the thin airfoils (i.e., producing up to 20.5% of the total thrust for NACA0004 airfoil in the present study). The role change of viscous force in the thrust generation of the plunging airfoils was found to be closely related to the dynamics of the unsteady vortex structures around the plunging airfoils.

References

[1] Knoller, R., "Die Gesetze des Luftwiderstandes," *Flug- und Motortechnik*, Vol. 3, No. 21, 1909, pp. 1–7.

[2] Betz, A., "Ein Beitrag zur Erklaerung des Segelfluges," *Zeitschrift fuer Flugtechnik und Motorluftschiffahrt*, Vol. 3, 1912, pp. 269–270.

[3] Katzmayr, R., "Effect of Periodic Changes of Angle of Attack on Behavior of Airfoils," NACA TM 147, 1922.

[4] Ober, S., "Note on the Kaztmayr Effect on Airfoil Drag," NACA TN 214, 1925.

[5] von Kármán, T., and Burgers, J. M., *Aerodynamic Theory: A General Review of Progress*, edited by W. F. Durand, Vol. 2, Springer, Berlin, 1935.

[6] Koochesfahani, M. M., "Vortical Patterns in the Wake of an Oscillating Airfoil," *AIAA Journal*, Vol. 27, 1989, pp. 1200–1205.
    doi:10.2514/3.10246

[7] Dickinson, M. H., Lehmann, F. O., and Sane, S. P., "Wing Rotation and the Aerodynamic Basis of Insect Flight," *Science*, Vol. 284, 1999, pp. 1954–1960.
    doi:10.1126/science.284.5422.1954

[8] Jones, K. D., Dohring, C. M., and Platzer, M. F., "Experimental and Computational Investigation of the Knoller–Betz Effect," *AIAA Journal*, Vol. 36, No. 7, 1998, pp. 1240–1246.
doi:10.2514/2.505

[9] Platzer, M. F., Jones, K. D., Young, J., and Lai, J. C. S., "Flapping-Wing Aerodynamics: Progress and Challenges," *AIAA Journal*, Vol. 46, No. 9, 2008, pp. 2136–2149.
doi:10.2514/1.29263

[10] Ashraf, M. A., Yong, J., and Lai, J. C. S., "Reynolds Number, Thickness and Camber Effects on Flapping Airfoil Propulsion," *Journal of Fluids and Structures*, Vol. 27, 2011, pp. 145–160.
doi:10.1016/j.jfluidstructs.2010.11.010

[11] Wang, Z. J., "Vortex Shedding and Frequency Selection in Flapping Flight," *Journal of Fluid Mechanics*, Vol. 410, 2000, pp. 323–341.
doi:10.1017/S0022112099008071

[12] Lewin, G. C., and Haj-Hariri, H., "Modeling Thrust Generation of a Two-Dimensional Heaving Airfoil in a Viscous Flow," *Journal of Fluid Mechanics*, Vol. 492, 2003, pp. 339–362.
doi:10.1017/S0022112003005743

[13] Shyy, W., Lian, Y., Tang, J., Viieru, D., and Liu, H., *Aerodynamics of Low Reynolds Number Flyers*, Cambridge Univ. Press, New York, 2008.

[14] Hu, H., Clemons, L., and Igarashi, H., "An Experimental Study of the Unsteady Vortex Structures in the Wake of a Root-Fixed Flapping Wing," *Experiments in Fluids*, Vol. 51, No. 2, 2011, pp. 347–359.
doi:10.1007/s00348-011-1052-z

[15] Yu, M. L., Wang, Z. J., and Hu, H., "A High-Order Spectral Difference Method for Unstructured Dynamic Grids," *Computers and Fluids*, Vol. 48, 2011, pp. 84–97.
doi:10.1016/j.compfluid.2011.03.015